

The possibility of using an autogenous Hydrogen-DRI slag as a raw material for vanadium extraction

Joar Huss¹, Amanda Vickerfält² and Niklas Kojola³ (initials and surnames only)

1. Researcher, Swerim AB, Isafjordsgatan 28A, 164 40, Stockholm, Sweden.

Email: joar.huss@swerim.se

2. Researcher, Swerim AB, Isafjordsgatan 28A, 164 40, Stockholm, Sweden.

Email: amanda.vickerfalt@swerim.se

3. Researcher, Hybrit Development AB, Klarabergsviadukten 70, E6, 101 21, Stockholm, Sweden,

Email: niklas.kojola@hybrit.se

Keywords: Fossil-free steel, Autogenous slag, Vanadium extraction, Phosphorus partition

ABSTRACT

The possibility of using an acidic autogenous hydrogen direct reduced iron (H-DRI) slag as a basis for vanadium extraction is investigated. For a raw material to be suitable for producing high-quality FeV, the vanadium oxide content should be sufficiently high and the phosphorus oxide content in a tolerable range. Therefore, the feasibility for vanadium extraction relies on fulfilling two demands: the predominate partitioning of phosphorus to the metal and vanadium to the slag. Correspondingly, the behaviors of phosphorus and vanadium in the $\text{Al}_2\text{O}_3\text{-SiO}_2\text{-FeO}_x\text{-V}_y\text{O}_z\text{-P}_2\text{O}_5\text{-Fe}$ system were studied experimentally. Slag, 10g, was put in contact with liquid iron, 30g, for different durations (2-24 h) in closed alumina crucibles at 1873 K. The slag composition was varied between 33.1-49.3 wt% Al_2O_3 , 27.1-46.7 wt% SiO_2 , 16.6-30.1 wt% FeO_x , and 2.5-8.8 wt% V_2O_3 . The equilibrium phosphorus distribution was 0.42, while the vanadium distribution ranged from 7.6 to 43.4, increasing with the Al_2O_3 - and the FeO_x -content.

INTRODUCTION

Ferro vanadium (FeV) is used to alloy steels of many grades during secondary steelmaking (Moskalyk, Alfantazi, 2003). The oxygen potential in this process step is intentionally kept very low to maximize the yield of the alloying element. The ability to refine steel from phosphorus is virtually non-existent in environments with low oxygen potential. Since phosphorus will contaminate the steel during secondary steelmaking, the quality of the alloying element is, among other factors, determined by its phosphorus content (Tao et al., 2020). Correspondingly, it is desirable to minimize the P-content in the FeV.

Converter slag has been seen as a largely untapped resource for vanadium production. The production of a high-quality, low phosphorus FeV from converter slag has therefore been of interest for previous studies, and while some innovative approaches have been proposed, none have seen industrial adoption (Lindvall et al, 2017) (Lindvall et al, 2010) (Gupta, Krishnamurthy, 1992). The main difficulty originates from the parallel transfer of vanadium and phosphorus from the liquid pig iron to the converter slag (Lindvall et al, 2017) (Lindvall et al, 2010). At the same time, it is challenging to remove phosphorus during the extraction process (Tao et al, 2020). The amount of phosphorus in a slag intended for V-extraction should, therefore, be minimized during steelmaking. The future fossil-free production route could offer an opportunity for this purpose. In the novel fossil-free production route, where hydrogen direct reduced iron (H-DRI) will be the principal material, the initial conditions are different compared to the blast-furnace route. In the H-DRI, vanadium and phosphorus are initially in oxide phases originating from the iron ore (Jonsson et al, 2013)(Lövgren, 2005). Vanadium is then concentrated in the autogenous slag during melting. Unfortunately, when fluxed, typically with CaO, the slag will also dephosphorize the steel made from H-DRI (Vickerfält, Martinsson, Sichen, 2021) (Huss, Berg, Kojola, 2020). A future autogenous slag must be specially engineered for a high V- and low P-content for feasible vanadium extraction. In other words, the autogenous slag should satisfy two demands for it to be suitable as raw material for vanadium extraction, viz., (a) the vanadium content should be sufficiently high, and (b) the phosphorus content should be in a tolerable range. The basis for a potential slag design is briefly outlined below.

The two main demands could be met by designing the autogenous slag for (a) a suitable oxygen potential during steelmaking and (b) a low dephosphorization power. Firstly, a suitable oxygen potential during steelmaking must be established to achieve the desired P and V distributions. Since the FeO content determines the oxygen potential, the FeO content in the slag should be designed. Secondly, the dephosphorization power of the slag is, in addition to the oxygen potential, dependent on the oxygen anion activity (Herasymenko, 1941). Correspondingly, a future autogenous slag should be engineered for a low oxygen anion activity to decrease the dephosphorization power of the slag. It is well established that the oxygen anion activity is strongly limited in acidic slag systems due to the high degree of structural linkage. Hence, in theory, an acidic slag could be a suitable basis for vanadium extraction. For efficient material use, the specially designed acidic autogenous slag should be based on the gangue found in the H-DRI. The main components of the gangue are silica and alumina (Lövgren, 2005) (LKAB Product Catalogue, 2021). Thus, the pseudo-quaternary $\text{Al}_2\text{O}_3\text{-SiO}_2\text{-FeO}_x\text{-V}_y\text{O}_z$ system is an interesting candidate to study, summarizing the outline.

Some previous studies have been carried out on related systems, viz., the $\text{CaO-Al}_2\text{O}_3\text{-V}_2\text{O}_3$ and the $\text{CaO-Al}_2\text{O}_3\text{-SiO}_2\text{-V}_2\text{O}_3$ systems (Lindvall, Gran, Sichen, 2014) (Vermaak, Pistorius, 2000). Vermaak and Pistorius (2000) found that the activity coefficient of vanadium(III)oxide in the liquid slag phase decreased substantially with increasing $\text{CaO/Al}_2\text{O}_3$ ratios. Lindvall et al (2014) observed that vanadium oxide was predominantly found in the solid phases of the slag, while the concentration in the liquid slag phase was close to 0 wt%. As the present system is hardly studied, this work presents novel and relevant results to determine whether an appropriately engineered autogenous H-DRI slag could provide new possibilities for vanadium extraction. Unfortunately, no commercial DR-grade pellets specially engineered for this purpose are available. The future possibility is, therefore, investigated by employing synthetic slags.

In summary, this exploratory study aims to assess the possibility of using an acidic autogenous slag as a raw material for vanadium extraction by investigating the distribution between relevant synthetic slags and liquid iron of (1) vanadium and (2) phosphorus and (3) by investigating the present slag phases to understand the behaviors better.

EXPERIMENTAL

Experimental setup

A vertical resistance heated tube furnace was employed to study the distributions and slag phases. A schematic drawing of the setup is given in **Figure 1**. The alumina reaction tube was fitted in the lower end with a water-cooled aluminum cap and in the upper end with an interconnected water-cooled aluminum cooling chamber. Argon gas (99.999% purity) was passed to the reaction tube through an inlet situated in the aluminum cap and led out through an outlet placed in the cooling chamber. The cooling chamber was equipped with an additional inlet to allow a separate high flow of argon gas to be injected directly into the cooling chamber to enhance the heat transfer from the sample during cooling. A B-type thermocouple with an outer alumina sheath was installed through a compression seal fitting in the aluminum cap and positioned close to the sample in the even temperature zone (± 4 K over 10 cm) to monitor the temperature. The samples were suspended in the furnace using an arrangement consisting of a lifting system, a steel tube, a Mo-tube, and a Mo-crucible holder. The steel tube was attached to the lifting system and entered the furnace through the cooling chamber. The upper end of an intermediate Mo-tube was connected to the steel tube, while a Mo-crucible holder was connected to the lower end. The Mo-crucible holder held one recrystallized double-sintered alumina crucible, 60 mm h \times 36 mm \varnothing at a time, in which the sample resided. The orifice of the crucible was covered with a Mo-lid, thus closing the system. The suspension arrangement was, in turn, connected to a lifting system, enabling the movement of the samples in the vertical direction. Additionally, simmerings were fitted to the steel rod. Thus, the atmosphere was prevented from being altered by the movement of the rod. A gas-tight seal of the reaction tube was ensured by sealing the other setup components using O-rings.

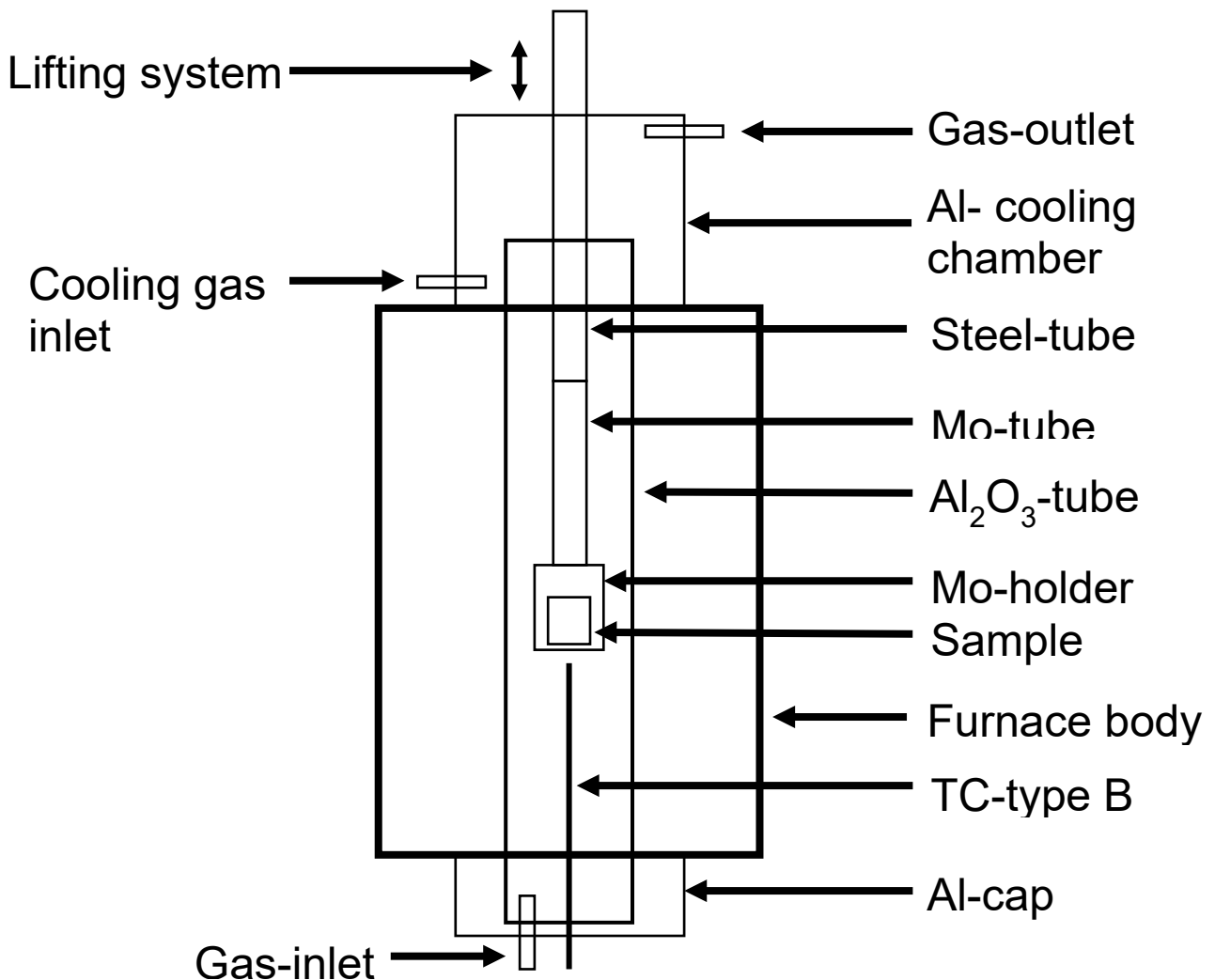


FIG 1 – Schematic drawing of the experimental setup

Sample preparation

The samples consisted of metal and slag. The metal phase was prepared by mixing 30 g of Fe- (99.9% purity) and Fe₃P-powder (99.5%) in an agate mortar. The total amount of phosphorus was varied by adding different amounts of Fe₃P and Fe. The corresponding P concentration, should all phosphorus commit to the metal phase, was thus varied between 0.1 to 0.82 wt%. The slag phase was prepared by mixing FeO_x and commercially available Al₂O₃ (99.97% purity), SiO₂ (99.5%), and V₂O₃ (99.7%) powders. FeO_x was made in-house by thoroughly mixing Fe-powder (99.9%) and Fe₂O₃-powder (99.9%) to an oxygen content of 51.4 at%, followed by sintering in a closed iron crucible at 1373 K for 8 h. An argon atmosphere protected the iron crucible from oxidation throughout the sintering. The Al₂O₃ and SiO₂ powders were heated to 1173 K for 72 h prior to usage. 10 g of the slag components were then mixed in an agate mortar for 15 min. Phosphorus was added to the slag side in one experiment, **Sample 10**, using Mg₂P₂O₇, to check the reliability of the experiments. Moreover, a specific procedure of adding the sample to the crucible was used to limit the reaction between the slag and the crucible during heating. A ~5 g portion of the Fe-mixture was first added to the crucible covering its base. The slag mixture was pressed into three cylindrical pellets using a hydraulic press and a steel die (23 mm ID) with an applied pressure of 30 MPa. The slag pellets were then stacked and centered in the crucible. Subsequently, the gap between the crucible wall and slag pellets was filled with the remaining Fe-mixture. Considering the limited contact between the slag and the crucible, the reaction between the two is expected to be minimized during heating. The system was then sealed by placing a polished Mo-lid on the crucible orifice, which was also polished beforehand. The weighed-in slag and metal compositions and the experimental durations are given in **Table 1**.

TABLE 1 – Weighed-in slag and metal compositions and the corresponding experimental durations. *P added as Mg₂P₂O₇ given as the corresponding [P]_{Fe} content.

Sample No.	Duration hours	Al ₂ O ₃ wt%	SiO ₂ wt%	FeO _x wt%	V ₂ O ₃ wt%	Al ₂ O ₃ /SiO ₂	[P] _{Fe} wt%
1	6	18.75	31.25	40.00	9.99	0.6	0.20
2	2	17.10	42.85	30.01	10.04	0.4	0.82
3	2	31.79	52.95	10.18	5.08	0.6	0.20
4	24	30.00	50.00	10.00	10.00	0.6	0.10
5	4	30.00	50.00	10.00	10.00	0.6	0.10
6	6	30.00	50.00	10.00	10.00	0.6	0.20
7	6	26.25	43.75	20.00	10.00	0.6	0.20
8	2	26.05	43.35	10.74	19.85	0.6	0.89
9	2	42.83	37.23	9.90	10.04	1.2	0.80
10	2	30.00	50.01	10.01	9.98	0.6	0.80*
11	2	29.99	49.93	10.06	10.01	0.6	0.81
12	2	10.00	49.78	30.16	10.08	0.2	0.81
13	2	50.25	29.52	10.33	9.91	1.7	0.82
14	2	54.42	24.70	11.05	9.84	2.2	0.82

Experimental procedure

The sample was mounted to the lifting system and suspended in the water-cooled aluminum chamber. The furnace was then sealed. The reaction tube was evacuated, and the seal was checked for vacuum. Argon gas was subsequently passed to the reaction tube to atmospheric pressure. The reaction tube was evacuated again and backfilled with argon gas. This process was repeated five times to ensure the desired atmosphere was acquired. A flow of 0.1 L min^{-1} was then kept throughout the experiment. The furnace was heated up to the experimental temperature of 1873 K at a rate of 1.7 K min^{-1} . The sample was preheated to avoid shocking the reaction tube by slowly lowering the sample to a preheating position (1573 K), followed by a 10-minute thermal equilibration period. The sample was then quickly lowered to the even temperature zone and kept for different durations, 2-24 h, see **Table 1**. After the experimental duration, the sample was raised to the aluminum cooling chamber in a matter of seconds, where a separate high flow of argon gas was injected to enhance the cooling. The furnace was then cooled down, and the sample was extracted. The slag was found attached to the crucible wall and needed to be mechanically separated by grinding the crucible wall before chemical analysis. After separation, the composition of the slag was analyzed using X-ray fluorescence (XRF), and the present phases were studied using a scanning electron microscope with supplementary energy dispersive spectroscopy (EDS) functionality. The metal phase released readily from the crucible and the slag. After separation, the metal composition was analyzed using optical emission spectroscopy (OES).

RESULTS

The phosphorus and vanadium distributions in the closed $\text{Al}_2\text{O}_3\text{-SiO}_2\text{-FeO}_x\text{-V}_2\text{O}_3\text{-Fe}$ system were studied as a function of slag composition. The compositions of the slag and the metal phase are given in **Table 2**. Omitted from the table are minor oxidic constituents, i.e., with a content of <0.2 wt%, except for P_2O_5 . Note that phosphorus was added to the slag side as $\text{Mg}_2\text{P}_2\text{O}_7$ in one experiment, **Sample 10**, resulting in a MgO content of 1.9 wt%. Moreover, the determination of valences was not within the scope of this work. The content of vanadium and iron oxide is, therefore, given in the Fe^{2+} and V^{3+} valence states even though the presence of multiple valences is likely (Wang, Li, Sichen, 2011) (Allertz, Selleby, Sichen, 2015). The P_2O_5 content was found to be low or below the detection limit for all slag compositions, **Table 2**, while the content of V_2O_3 varied between 2.5-8.8 wt%. The distributions of P and V between slag and metal were calculated by virtue of equations (1) and (2), respectively, to further the examination.

$$L_P = \frac{2M_P \times (\text{wt}\% \text{P}_2\text{O}_5)}{M_{\text{P}_2\text{O}_5} \times [\text{wt}\% \text{P}]_{\text{Fe}}} \quad (1)$$

where L_P is the phosphorus distribution between slag and metal, (wt% P_2O_5) the analyzed content of phosphorus oxide in the slag phase, $[\text{wt}\% \text{P}]_{\text{Fe}}$ the analyzed concentration of phosphorus in the metal phase, and M_P , $M_{\text{P}_2\text{O}_5}$ the molar masses of phosphorus and phosphorus oxide respectively.

$$L_V = \frac{2M_V \times (\text{wt}\% \text{V}_2\text{O}_3)}{M_{\text{V}_2\text{O}_3} \times [\text{wt}\% \text{V}]_{\text{Fe}}} \quad (2)$$

where L_V is the vanadium distribution between slag and metal, (wt% V_2O_3) the analyzed content of vanadium oxide in the slag phase, $[\text{wt}\% \text{V}]_{\text{Fe}}$ the analyzed concentration of vanadium in the metal phase, and M_V , $M_{\text{V}_2\text{O}_3}$ the molar masses of vanadium and vanadium oxide respectively.

The L_P was calculated for **Samples 4** and **10** to 0.42 and 0.40, respectively, while the L_V varied between 7.6 and 43.4. The calculated distributions are given together with the respective slag compositions in **Table 2**.

TABLE 2 – Analysis of the slag (XRF), metal phase (OES), and present phases.

Sample No.	XRF					$\text{Al}_2\text{O}_3/\text{SiO}_2$	OES		L_V	L_P	Phases
	Al_2O_3 wt%	SiO_2 wt%	FeO_x wt%	V_2O_3 wt%	P_2O_5 wt%		$[\text{P}]_{\text{Fe}}$ wt%	$[\text{V}]_{\text{Fe}}$ wt%			
1	38.2	27.3	30.1	4.4	<0.01	1.40	0.159	0.069	43.4		S, L
2	36.6	33.4	24.8	5.2	<0.01	1.09	0.297	0.144	24.6		S, L
3	33.3	46.7	17.5	2.5	<0.01	0.71	0.300	0.223	7.6		M, L
4	37.1	39.3	18.2	5.3	0.082	0.95	0.085	0.380	9.5	0.42	S, L, M
5	33.4	42.3	18.7	5.6	<0.01	0.79	0.090	0.390	9.7		S, L, M
6	35.2	42.6	16.8	5.4	<0.01	0.82	0.174	0.419	8.8		S, L, M
7	40.0	34.2	20.3	5.4	<0.01	1.17	0.154	0.234	15.5		S, L, M
8	37.9	31.3	21.9	8.8	<0.01	1.21	0.300	0.329	18.2		S, L, M
9	43.5	32.8	17.1	6.6	<0.01	1.33	0.289	0.309	14.5		S, L, M
10	36.6	37.1	20.8	5.2	0.265	0.99	0.288	0.208	16.8	0.40	S, L, M
11	33.1	43.8	17.6	5.5	<0.01	0.76	0.299	0.422	8.9		S, L, M
12	37.1	34.0	23.8	5.1	<0.01	1.09	0.293	0.175	19.7		S, L, M
13	48.3	28.3	16.6	6.8	<0.01	1.71	0.298	0.221	20.8		S, L, M, C
14	49.3	27.1	16.9	6.7	<0.01	1.82	0.300	0.153	29.7		S, L, M, C

Furthermore, it was found that the vanadium distribution increased with an increase in the FeO- and in the Al₂O₃ content. To ease the detailed examination, L_V is shown as a function of the FeO content in **Figure 2(a)**. As indicated in the figure, the slag compositions have been divided into subsets of similar mass ratios of Al₂O₃/SiO₂. In **Figure 2(b)**, L_V is given as a function of the Al₂O₃/SiO₂ ratio for slags with similar FeO contents. By examining the figures, it is clear that the vanadium distribution increases with increasing contents of FeO and with increasing Al₂O₃/SiO₂ mass ratios.

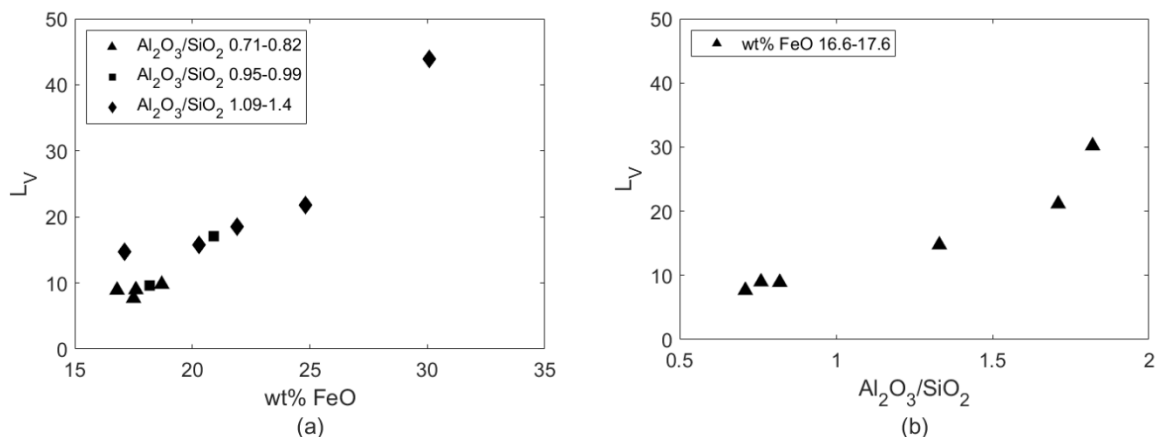


FIGURE 2 – L_V as a function of (a) the FeO content and (b) the Al₂O₃/SiO₂ mass ratio

Further, the L_V data can be used to estimate the vanadium oxide content in an autogenous slag where the H-DRI is based on an iron ore with a vanadium(V)oxide content of 0.25 wt%. A mass balance approach was used for the calculation where the slag-to-metal mass ratio was varied between 3 and 4.2% depending on the amount of alumina needed to modify the autogenous slag and the mass of FeO. It is calculated that the vanadium oxide content could vary between 2 and 5.5 wt%. The estimated vanadium oxide content in the autogenous slag is given as a function of FeO in **Figure 3**, where some relevant examples of the Al₂O₃/SiO₂ mass ratios are given next to the data points.

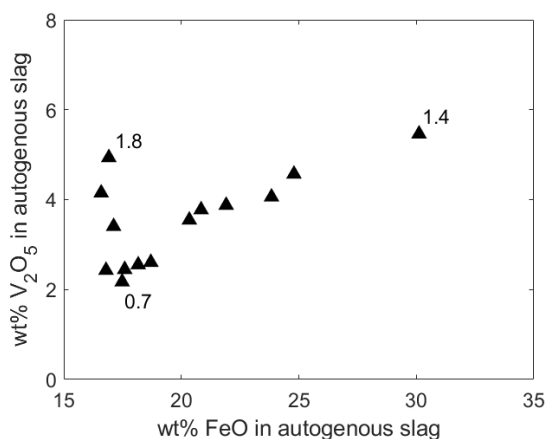


FIGURE 3 – Calculated vanadium oxide content in the autogenous slag as a function of FeO content.

The present slag phases were examined to better understand the effect of Al₂O₃ and FeO on L_V. When analyzed by SEM-EDS, a total of four different phases were found: spinel phase, "S", liquid phase, "L", mullite phase, "M", and corundum phase, "C". The phases present in each sample are given in **Table 2**. As the table shows, four different phase relations were encountered: L-S, L-M, L-S-M, and L-S-M-C. **Figures 4(a)-(d)** show an example micrograph of each phase relationship.

A microstructure consisting of two phases, a liquid phase (grey) and a vanadium-containing spinel phase (light grey), was found in slags with a FeO content of 27.5 +/- 2.6 wt% (**Samples 1, 2**) **Figure 4(a)**. A different microstructure containing a liquid- (grey) and a mullite phase (dark grey) was found for a slag containing 17.5 wt% FeO, **Sample 3**, see **Figure 4(b)**. For slags containing 33.1- 43.4 wt% Al₂O₃, 31.3- 43.7 wt% SiO₂, and 16.8 -21.9 wt% FeO_x (**Samples 4- 12**), a microstructure containing three phases, the bright spinel phase, the angular dark grey mullite, and the grey liquid phase was found, see **Figure 4(c)**. For slags containing 47.5- 48.3 wt% Al₂O₃ (**Samples 13, 14**), the Al-corundum phase was present in addition to the previously mentioned phases; see **Figure 4(d)**. Furthermore, it was found that the composition of the phases varied depending on the total slag composition. Given the uncertainties associated with EDS analysis, the composition of the present phases for all slag compositions is not reported. Instead, to illustrate the composition of the present phases, the EDS analysis of the phases for one sample containing all phases, **Sample 13**, is provided in **Table 3**.

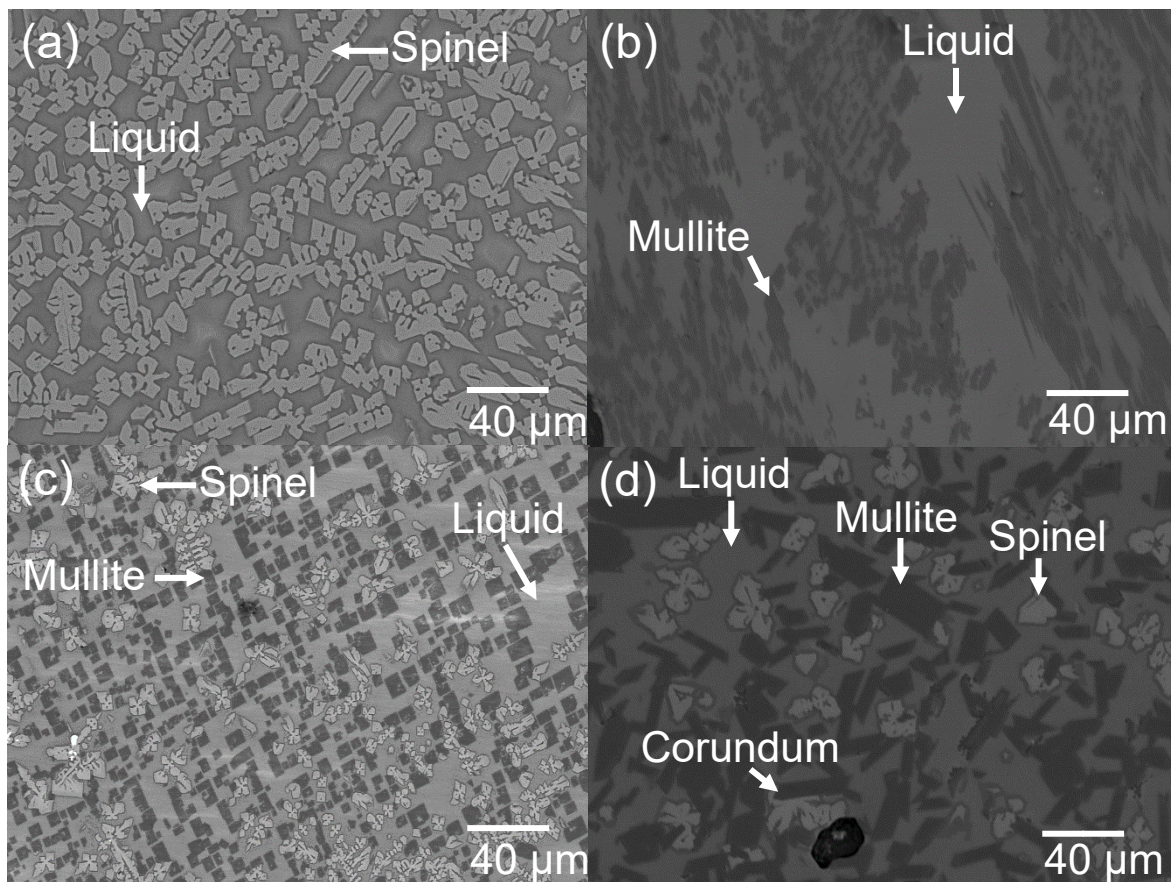


FIGURE 4 – Microstructures containing (a) the liquid- and spinel phase, (b) the liquid- and mullite phase, (c) the liquid-, mullite- and spinel phase, and (d) in addition the corundum phase.

TABLE 3 – Example of phase compositions by EDS.

Phase	Al ₂ O ₃ wt%	SiO ₂ wt%	FeO _x wt%	V ₂ O ₃ wt%
Spinel	40.3	3.3	35.3	21.1
Liquid	18.8	52.2	28.9	0.1
Mullite	60.6	28.6	1.2	9.6
Corundum	86.9	0	1.0	12.1

DISCUSSION

Phosphorus distribution

The distribution expression in equation (1) is, to some extent, dependent on the ratio of slag to metal mass. For practical convenience, the ratio of slag to metal in the present study was set to 1:3, while the ratio is commonly around 1:6-10 in the EAF (Horii et al, 2013). In remedy, a far greater concentration of phosphorus than expected in the industry was employed. The phosphorus oxide content in the slag will, therefore, be exaggerated in this experimental study compared to industrial conditions. Despite this fact, the phosphorus content in the slag was low or below the detection limit. This shows that the experimental observations would apply to the industrial case even though the slag-to-metal ratio is different.

Sample 4 was kept for 24 h, which is considerably longer than needed to establish equilibrium between metal and slag (Basu, Lahiri, Seetharaman, 2007) (Suito, Inoue, Takada, 1981). Therefore, the observed phosphorus partition is considered the equilibrium distribution. The phosphorus content at equilibrium was 0.1 wt% with an L_P of 0.42, whereas the content was below the detection limit for slags kept at a shorter duration. The difference indicates that equilibrium was not established during the shorter experimental time. Regardless, the very low phosphorus contents in the slag show that its dephosphorization power is undoubtedly low. This is expected considering the low oxygen anion activity in acidic slags. Additionally, phosphorus was added to the slag side in one experiment, **Sample 10**. The experimental duration was 2 h, which resulted in a phosphorus distribution of 0.40. This is similar to **Sample 4** (0.42), which indicates that phosphorus initially in the slag phase is transferred at a faster rate to the metal phase than vice versa. Potentially, this is an aspect that should be considered in industrial applications. Nevertheless, it is evident that the proposed slag system is efficient in partitioning phosphorus to the metal phase, which unconventionally is the desired outcome. One of the necessary conditions for the possible vanadium extraction from an autogenous slag of the present slag system is thereby met. The second condition is the predominant partitioning of vanadium to the slag phase.

Behavior of vanadium

The vanadium content in the autogenous slag must be sufficiently high for feasible vanadium extraction. Ultimately, the vanadium oxide concentration in the ore determines V-content in the slag and, thereby, whether the autogenous slag can feasibly be used for vanadium extraction. The feasibility should correspondingly be evaluated based on the ore. For this purpose, the vanadium oxide content in the autogenous slag was estimated based on the experimentally determined L_V and an iron ore containing 0.25 wt% of vanadium(V)oxide (LKAB Product Catalogue, 2021). It is estimated that the vanadium oxide content in the autogenous slag could vary between 2 wt% and 5.5 wt%, **Figure 3**. A vanadium content of 2 wt% is likely less than needed for an economically feasible extraction today, while 5.5 wt % could constitute, for this purpose, a sufficient portion of the slag.

Both demands have been satisfied since phosphorus is predominantly partitioned to the metal and the autogenous slag could contain a significant vanadium oxide content. It is, therefore, possible that an autogenous H-DRI slag based on the present system could provide a new opportunity for vanadium extraction. Further, to aid in the future process design, the behavior of vanadium is discussed in detail based on the phases in the slag. The main focus of the discussion is given to the effect of slag composition and the impact of oxygen potential.

Vanadium-containing slag phases

To help the discussion in the later section, the phases in the slag will be discussed first. The present phases were identified based on the respective compositions. The mullite phase is of the $3Me_2O_3:2MeO_2$ form, corresponding to a molar ratio of Me^{3+} to Me^{+4} of 1.5 (Schneider, Schreuer, Hildmann, 2008). It is reasonable to assume that solid solution could lead to a shift in the ratio. For this reason, some thermodynamic calculations were carried out in the Al-Si-O system, which showed that the ratio between Me^{3+} and Me^{+4} can vary between 1.38 and 1.77 (Andersson et al., 2002). The observed ratio, specifically the $(Al_2O_3+V_2O_3)/SiO_2$ molar ratio, was 1.38, see **Table 3**, and is thus in line with the calculated boundaries. In addition, around 1-2 wt% of FeO_x was detected in the mullite

phase, which could come from background interference in EDS analysis. This, nevertheless, shows that the amount of Me^{2+} lattice positions is limited, in line with the established understanding of the mullite phase (Schneider, Schreuer, Hildmann, 2008).

A similar approach was employed in identifying the spinel phase. The spinel phase consists of alumina, iron-, and vanadium oxide. By not allowing silica, Si^{4+} , into the lattice, it is concluded that the Me^{4+} positions are limited, in line with the established understanding of the 2-3 spinel structure (Tsurkan et al, 2021). The measured phase composition also agreed with the V-Fe-Al-O phase diagram (Slag Atlas, 2020), further supporting the argument. Moreover, vanadium was found almost exclusively in the solid phases of the slag, see **Table 3**, which is similar to what Lindvall et al (2014) observed for a related slag system. This could be due to the activity coefficient of vanadium(III)oxide being significantly higher in the acidic liquid slag phase than in the solid phases (Vermaak, Pistorius, 2000). A systematic study regarding the activity coefficients of vanadium(III)oxide in the different phases is needed to explain this phenomenon fully. Further, it is noted that the spinel phase was suppressed as the content of vanadium oxide in the system was low, **Sample 3, Figure 4(b)**, and that the mullite phase did not form at higher FeO contents, **Samples 1 and 2, Figure 4(a)**. The principal vanadium-carrying phase could, therefore, depend on the ingoing material and the used praxis. Considering that the difference in the present phases will likely impact the subsequent vanadium extraction process, it is essential to consider the phases together with the employed praxis. The corresponding phase diagrams of the spinel, mullite, and corundum phases and the respective roasting and leaching properties will be integral to study to orientate a future process better.

Vanadium distribution

Effect of vanadium oxide content on L_V

The effect of vanadium oxide content on the vanadium distribution between slag and metal was investigated by varying the amount of added V_2O_3 . **Samples 7 and 8** contained similar alumina to silica ratios and FeO contents, while the final V_2O_3 content differed (5.4-8.8 wt%). A similar distribution of vanadium was observed for the samples (15.5 and 18.2). This shows that the amount of V_2O_3 in the system does not profoundly change the vanadium distribution in the system over the mentioned range. Similarly, **Samples 3 and 5** display a similar behavior over the final V_2O_3 content range of 2.5-5.6 wt%. This shows that a variation in V_2O_3 content in a small range does not profoundly impact the vanadium distribution of the system. In contrast, when the full range of final V_2O_3 contents (2.5-8.8 wt%) is examined, there is a measurable difference. As vanadium is added to the slag side, a portion of the vanadium is reduced and dissolved in the metal phase. In the closed system, the chemical potentials are set by the ingoing components, which means the reduction of vanadium is achieved by the parallel oxidation of iron. This leads to a dynamic stabilization of the chemical potentials where the FeO concentration initially increases and is followed by the dissolution of the crucible material (Slag Atlas Version 16, 2020). Hence, the stabilization of the potentials results in an increase in the alumina-to-silica ratio, which significantly impacts the vanadium distribution.

Effect of alumina to silica ratio and FeO on L_V

The ability to vary the silica-to-alumina ratio is limited under the equilibrium condition. Therefore, to investigate the distribution of vanadium over a broader range of compositions, a duration of 2 h was chosen for most of the experiments. To ensure the experiments can be used for semi-quantitative determination of V and P distributions, four separate experiments were carried out where the distributions were examined over a duration range of 2-24 hours, **Samples 4, 5, 6, and 11**. No profound change in the distribution of vanadium and phosphorus was apparent over the duration range. This strongly suggests that the results obtained over a 2-hour experimental duration will be suitable for semi-quantitative determination of the distribution of vanadium at different $\text{Al}_2\text{O}_3/\text{SiO}_2$ ratios.

Due to the dissolution of the crucible material, it is not possible to quantitatively distinguish the effect of FeO_x from the impact of the alumina to silica ratio ($\text{Al}_2\text{O}_3/\text{SiO}_2$) on L_V . The effects are, therefore, discussed separately in a qualitative manner. With increasing FeO contents, the FeO activity will increase, resulting in a higher oxygen potential. The increase in the partial pressure of oxygen will drive the oxidation reaction of vanadium, equation (3), to the right-hand side, thus increasing L_V . The

effect is evident when examining **Figure 2(a)**, where the vanadium distributions of similar ratios of Al_2O_3/SiO_2 are shown as a function of the FeO_x content.



In addition, it is clear from **Figure 2(b)** that an increase in the Al_2O_3/SiO_2 ratio has resulted in an increase in the vanadium distribution. Principally, two mechanisms operate simultaneously, resulting in the observed effect. The first is related to the oxygen potential in the system, and the second is the varying fraction of the solid phase. Considering the mechanisms operate simultaneously and interdependently, they will be discussed together. As a first step in the discussion, only the mullite phase is considered.

Systems with higher Al_2O_3/SiO_2 ratios will contain a larger fraction of mullite phase than systems with a lower ratio. As the solubility of FeO in mullite is very low, for any given FeO concentration, the liquid slag phase of high-ratio systems will contain more FeO and have higher oxygen potential compared to the corresponding low-ratio systems. To support the argument, the activity of FeO, at a fixed FeO content, of slags in equilibrium with liquid iron was calculated as a function of the Al_2O_3/SiO_2 ratio for the Al-Si-Fe-O system, using a commercial thermodynamic software (Andersson, 2002). The FeO activity for a high-ratio system (1.6) was double that of a low-ratio system (0.6), see **Table 4**. As discussed, the higher FeO-activity will, in turn, result in a higher oxygen potential. The corresponding oxygen potentials were, therefore, calculated by virtue of equations 4- 6 and are also presented in **Table 4** (Basu, Lahiri, Seetharaman, 2007). This ultimately entails that a higher Al_2O_3/SiO_2 ratio drives the oxidation reaction of V, thus increasing L_V .



with the corresponding free energy function:

$$\Delta G^\circ = -256061 + 53.831 \times T \left(\frac{J}{mole} \right) \quad (5)$$

where the equilibrium constant is defined as:

$$K = \frac{a_{FeO}}{a_{Fe} \times p_{O_2}^{1/2}} \quad (6)$$

where K is the equilibrium constant of equation (6), a_{FeO} is the activity of FeO, a_{Fe} the activity of iron and p_{O_2} the partial pressure of oxygen.

TABLE 4 – Calculated oxygen potential as a function of the Al_2O_3/SiO_2 ratio of the slag in equilibrium with liquid iron at 1873K for the Al-Si-Fe-O system.

Al_2O_3 wt%	SiO_2 wt%	FeO wt%	Al_2O_3/SiO_2	Mullite phase fraction	a_{FeO}	p_{O_2} atm
33.75	56.25	10.00	0.6	0.056	0.056	6.48E-12
45.00	45.00	10.00	1	0.241	0.072	1.07E-11
57.00	33.00	10.00	1.7	0.450	0.113	2.64E-11

To further the discussion, the spinel phase is also considered. Unfortunately, no detailed and reliable thermodynamic description of the vanadium-containing spinel was available. The effect of the fraction of spinel phase on the oxygen potential is therefore discussed qualitatively. The higher oxygen potential due to the mullite phase fraction could, to some extent, be lessened should the spinel phase also be present. The spinel phase consisted of alumina, iron-, and vanadium oxide. It is, therefore, expected that systems with a relatively high $\text{Al}_2\text{O}_3/\text{SiO}_2$ ratio will also contain a larger fraction of spinel phase compared to the low ratio system. The spinel phase contains a similar iron oxide content as the liquid phase, while the Al_2O_3 content is higher, see **Table 3**. Higher spinel phase fractions will, therefore, lead to the liquid phase containing more silica, which will, correspondingly, lower the FeO concentration in the liquid. It should be kept in mind that V is almost exclusively found in the solid phases of the slag. A higher fraction of solid phase(s) means the number of available lattice positions that vanadium can occupy is greater. More vanadium is allowed into the slag, resulting in a higher vanadium distribution between slag and metal. This reasoning implies that the highest vanadium distribution will be found at the highest total content of FeO and the highest $\text{Al}_2\text{O}_3/\text{SiO}_2$ ratio. The present reasoning is, therefore, in line with the experimental results.

While it is important to consider the vanadium distribution in the industrial implementation, it should be considered together with other aspects, such as the physical properties of the slag, reaction kinetics, and the content of V, especially. Apart from the concentration of V in the ore, when a substantial amount of alumina and FeO_x is present in the slag, V could be diluted to the detriment of the subsequent extraction process, even though the L_V is relatively high. Correspondingly, it is essential to consider the L_V and the dilution effect simultaneously to optimize the V_yO_z content in the slag. Slags with high contents of vanadium oxide would, therefore, be an interesting topic for further studies.

SUMMARY

The possibility of using $\text{Al}_2\text{O}_3\text{-SiO}_2\text{-FeO}_x\text{-V}_y\text{O}_z$ slags as a basis for vanadium extraction was investigated. The possibility was evaluated based on the fulfillment of two overarching criteria: the predominant phosphorus partitioning to the metal phase and vanadium to the slag phase. It was found that the dephosphorization power of the slag was very low, with nearly all phosphorus partitioned to the metal phase. A significant amount of vanadium was kept in the slag, found almost exclusively in the solid phases. The distribution of vanadium increased with increasing ratios of $\text{Al}_2\text{O}_3/\text{SiO}_2$ and with increasing contents of FeO_x . The increase was discussed based on the oxygen potential in the system, the different vanadium-bearing solid phases, the fraction of solid phase, and the interplay between the fraction of solid phases and the oxygen potential. Ultimately, it was concluded that the studied slag system is a promising candidate for vanadium extraction as both criteria were satisfactorily met.

ACKNOWLEDGEMENTS

The authors gratefully acknowledge the financial support of HYBRIT Development AB.

The authors would like to express their gratitude to Prof. Pär Jönsson for his support. Also, we would like to express our most sincerest of thanks to Prof. Du Sichen for his never wavering patience in all discussions.

REFERENCES

- Allertz, C, Selleby, M, and Sichen, D, 2015. "Sulfide Capacity in Ladle Slag at Steelmaking Temperatures", Metallurgical and Materials Transactions B, 2609:2615-46(6)
- Andersson, J, Helander, T, Höglund, L, Shi, P and Sundman, B, 2002. "Thermo-Calc & DICTRA, computational tools for materials science", Calphad, 273:312-26
- Basu, S, Lahiri, A, Seetharaman, S, 2008. "Activity of Iron Oxide in Steelmaking Slag", Metallurgical and Material Transactions B, 357:366-38B(3)
- Basu, S, Lahiri, A and Seetharaman, S, 2007. "Phosphorus partition between liquid steel and CaO-SiO₂-FeOx-P₂O₅-MgO slag containing 15 to 25 Pct FeO", Metallurgical and Material Transactions B, 623:630-38B
- Gupta, C and Krishnamurthy, N, "Extractive Metallurgy of Vanadium", Elsevier Science Publishers B, AE Amsterdam, The Netherlands, 1992
- Herasymenko, P, 1941. "Fremdionen-Wirkung auf die Gleichgewichte zwischen Stahl und flüssigen Schlacken", Zeitschrift für Elektrochemie, 588:594-47(8)
- Horii, K, Tsutsumi, N, Kitano, Y and Kato, T, 2013. "Processing and Reusing Technologies for Steelmaking Slag", Nippon Steel Technical Report No. 104, 123:129
- Huss, J, Berg, M and Kojola, N, 2020. "Experimental Study on Phosphorus Partitions Between Liquid Iron and Liquid Slags Based on DRI", Metallurgical and Material Transactions B, 786:794-51B
- Jonsson, E, Troll, V, Högdahl, K, Harris, C, Nilsson, K and Skelton A, 2013. "Magmatic origin of giant 'Kiruna-type' apatite-iron-oxide ores in central Sweden", Scientific Reports, 1:8-3(1)
- Lindvall, M, Gran, J and Sichen, D, 2014. "Determination of the vanadium solubility in the Al₂O₃-CaO (25 mass%)-SiO₂ system", CALPHAD, 50:55-47
- Lindvall, M, Rutqvist, E, Ye, G, Björkvall, J and Sichen, D, 2010. "Possibility of Selective Oxidation of Vanadium from Iron and Phosphorus in Fe-V-P Melt", Steel Research International, 105:111-8(2)
- Lindvall, M, Tikka, J, Berg, M, Ye, G and Sichen, D, 2017. "Vanadium Extraction from a Fe-V (2.0 Mass%)-P (0.1 Mass%) Melt and Investigation of the Phase Relations in the Formed FeO-SiO₂-Based Slag with 20 Mass% V", Journal of Sustainable Metallurgy, 808:822-3
- LKAB Product Catalogue, 2021
- Lövgren, J, Master Thesis ISSN: 1402-1617, Luleå University of Technology, 2005
- Moskalyk, R and Alfantazi, A, 2003. "Processing of vanadium: a review", Minerals Engineering 793:805-16(9)
- Schneider, H, Schreuer, J and Hildmann, B, 2008. "Structure and properties of mullite-A review", Journal of the European Ceramic Society, 329:344-28
- Slagatlas, Version 16, GTT- Technologies, 2020
- Suito, H, Inoue, R and Takada, M, 1981. "Phosphorus Distribution between Liquid Iron and MgO Saturated Slags of the System CaO-MgO-FeOx-SiO₂", Transactions of the Iron and Steel Institute of Japan, 250:259-21
- Tao, C, Yu, Q, Liu, Z, Peng, Y, He, W and Deng, R, 2020. "Directional conversion and removal of complex phosphorus compounds from acidic leaching solution containing vanadium", Journal of Water Process Engineering, 1:8-37
- Tsurkan, V, Krug von Nidda, H, Deisenhofer, J, Lunkenheimer, P and Loidl, A, 2021. "On the complexity of spinels: Magnetic, electronic, and polar ground states", Physics Reports, 1:86-926
- Vermaak, M, Pistorius, P, 2000. "Equilibrium slag losses in ferrovanadium production", Metallurgical and Material Transactions B, 1091:1097-31B
- Vickerfält, A, Martinsson, J and Sichen, D, 2021. "Effect of Reduction Degree on Characteristics of Slag Formed by Melting Hydrogen-Reduced DRI and Partitions of P and V between Slag and Metal", Steel Research International, 1:11-92(3)
- Wang, H, Li, F and Sichen, D, 2011. "Development of an Analytical Technique to Determine the Fractions of Vanadium Cations with Different Valences in Slag", Metallurgical and Material Transactions B, 9:12-42